Biochem. J. (2012) 444, 211-218 (Printed in Great Britain) doi:10.1042/BJ20120074

world of information who



## Involvement of TSSA (trypomastigote small surface antigen) in Trypanosoma cruzi invasion of mammalian cells<sup>1</sup>

Gaspar E. CÁNEPA\*, Maria Sol DEGESE†, Alexandre BUDU‡, Celia R. S. GARCIA‡ and Carlos A. BUSCAGLIA\*<sup>2</sup>

\*Instituto de Investigaciones Biotecnológicas-Instituto Tecnológico de Chascomús (IIB-INTECh), Universidad Nacional de San Martín (UNSAM)—CONICET, Av. Gral Paz y Albarellos, Predio INTI, Edificio 24, San Martín, Buenos Aires, Argentina, †Instituto de Fisiología, Biología Molecular y Neurociencias (IFIBYNE), Facultad de Ciencias Exactas y Naturales, Universidad de Buenos Aires (UBA)—CONICET, Intendente Güiraldes 2160, Pabellón 2, Ciudad Universitaria, Buenos Aires, Argentina, and ‡Universidade de São Paulo, Departamento de Parasitologia, Instituto de Biociências, Cidade Universitária, 05508-900 São Paulo, Brazil

TSSA (trypomastigote small surface antigen) is a polymorphic mucin-like molecule displayed on the surface of Trypanosoma *cruzi* trypomastigote forms. To evaluate its functional properties, we undertook comparative biochemical and genetic approaches on isoforms present in parasite stocks from extant evolutionary lineages (CL Brener and Sylvio X-10). We show that CL Brener TSSA, but not the Sylvio X-10 counterpart, exhibits dosedependent and saturable binding towards non-macrophagic cell lines. This binding triggers Ca<sup>2+</sup>-based signalling responses in the target cell while providing an anchor for the invading parasite. Accordingly, exogenous addition of either TSSA-derived peptides or specific antibodies significantly inhibits invasion of CL Brener, but not Sylvio X-10, trypomastigotes. Non-infective epimastigote forms, which do not express detectable levels of TSSA, were stably transfected with TSSA cDNA from either parasite stock. Although both transfectants produced a surfaceassociated mucin-like TSSA product, epimastigotes expressing CL Brener TSSA showed a  $\sim$  2-fold increase in their attachment to mammalian cells. Overall, these findings indicate that CL Brener TSSA functions as a parasite adhesin, engaging surface receptor(s) and inducing signalling pathways on the host cell as a prerequisite for parasite internalization. More importantly, the contrasting functional features of TSSA isoforms provide one appealing mechanism underlying the differential infectivity of T. cruzi stocks.

Key words: calcium, cell invasion, mucin, Trypanosoma cruzi, trypomastigote small surface antigen (TSSA).

#### INTRODUCTION

Over 100 years after the discovery of its causative agent, the protozoan Trypanosoma cruzi, Chagas' disease remains the most important parasitic disease in the Americas, with an estimated toll of 50000 new cases per year [1]. Since this parasite often establishes life-long infection in humans, parasite transmission by contaminated blood is also becoming an important health issue in non-endemic countries. The toxicity and low effectiveness of therapy's approved drugs together with the absence of vaccines determine that the main control strategy for Chagas' disease still relies on the prevention of parasite transmission [2]. However, this is a complex zoonosis involving multiple haematophagous triatomine vectors, a wide range of wild and domestic mammals that serve as parasite reservoirs, and a very complex parasite population, which is likely to be the result of a predominantly clonal mode of evolution through large time spans [3]. Typing schemes based on biochemical and genetic markers converged in the delineation of six major intra-species evolutionary lineages termed TcI and TcIIa-TcIIe, which were recently renamed TcI-TcVI [4]. Importantly, biological variability displayed by T. cruzi stocks and different clinical manifestations of Chagas' disease have been partially correlated with parasite genetic diversity [5,6].

One critical step in the *T. cruzi* life cycle is the invasion of mammalian cells. This process has been studied extensively in vitro using a variety of cell types and either metacyclic trypomastigotes differentiated in axenic culture or cell-derived trypomastigotes as counterparts of insect-borne and bloodstream parasites respectively. The picture emerging from these studies suggests a rather complex, active and multi-step invasion phenomenon [7– 9]. Live-cell imaging studies revealed that parasites spend several minutes at a particular region of the target cell surface, where they appear to be probing for appropriate binding partners or to receive/transmit specific signals, before committing to invasion [7–9]. Indeed, Ca<sup>2+</sup> mobilization and other signalling cascades involving MAPKs (mitogen-activated protein kinases), protein phosphatases, phospholipases, cAMP and TGF $\beta$  (transforming growth factor  $\beta$ ) have been verified in parasites and/or mammalian cells upon contact [7–9]. Within the host cell, parasite-induced Ca<sup>2+</sup> signals promote localized fusion of lysosomes with the plasma membrane at the parasite attachment site, thus providing membrane for formation of the parasitophorous vacuole in which the parasite resides early after internalization [10].

The initial recognition/sensitization of the host cell involves various apparently redundant GPI (glycosylphosphatidylinositol)-anchored molecules belonging to the TS (transsialidase) protein family [7,8,11]. It was shown that cell-derived trypomastigote-restricted TS, Tc-85 and gp (glycoprotein) 83 bind to integrins, nerve growth factor receptor TrkA (tropomyosin receptor kinase A) and constituents of the extracellular

Abbreviations used: Ab, antibody; DAPI, 4',6-diamidino-2-phenylindole; DMEM, Dulbecco's modified Eagle's medium; ERK, extracellular-signalregulated kinase; FBS, fetal bovine serum; gp, glycoprotein; GPI, glycosylphosphatidylinositol; GST, glutathione transferase; HBSS, Hanks balanced salt solution; hEGF, human endothelial growth factor; HEK, human embryonic kidney; HRP, horseradish peroxidase; IFA, indirect immunofluorescence assay; mAb, monoclonal Ab; MAPK, mitogen-activated protein kinase; MEM, minimal essential medium; PI-PLC, phosphatidylinositol-specific phospholipase C; RT, reverse transcription; SP, signal peptide; TS, trans-sialidase; TSSA, trypomastigote small surface antigen; UTR, untranslated region.

The cDNA sequence data reported for trypomastigote small surface antigen I (TSSA I) have been deposited in the DDBJ, EMBL, GenBank® and GSDB Nucleotide Sequence Databases under accession number JQ354939.

This paper is dedicated to the memory of Dr Rodolfo Ugalde.

<sup>&</sup>lt;sup>2</sup> To whom correspondence should be addressed (email cbusca@iib.unsam.edu.ar).

matrix such as fibronectin and laminin [11–13], whereas metacyclic trypomastigote-restricted gp82 engage epithelial mucins [14]. Additional TS-related molecules including gp90 and gp30 participate in metacyclic trypomastigote attachment by recognizing as-yet undefined receptors on the host cell surface [7]. Mucin-like proteins, i.e. surface glycoproteins in which the oligosaccharide chains are O-glycosidically linked to threonine or serine residues, were also shown to be a driving force in host cell recognition and Ca2+ signalling, chiefly by means of their associated oligosaccharides [7,15-17]. Additional surface molecules contributing to parasite invasiveness have been described [18,19]. Adhesion properties from all of these parasite molecules were initially deduced from direct binding assays to whole cells, and from experiments in which parasite attachment/internalization was modulated by exogenous addition of soluble molecules, i.e. native/recombinant proteins, specific Abs (antibodies)/Fab fragments or glycosyl hydrolases able to interfere with ligand-receptor pairing. Even though the specifics do vary with each unique combination of parasite stock and host cell type, a rather common theme is that cell-derived trypomastigote surface adhesins, in contrast with metacyclic trypomastigote-derived ones, appear to rely on additional parasite enzymes to trigger Ca<sup>2+</sup> fluxes and other signalling cascades in the target cell [9,10,20].

In a previous paper, we described a small mucin-type protein termed TSSA (trypomastigote small surface antigen) displayed on the surface of cell-derived trypomastigote forms [21]. Two major TSSA isoforms were originally recognized: TSSA I present in TcI parasite stocks and TSSA VI (previously TSSA II) present in TcVI (previously TcIIe) isolates. Minor sequence variations between both isoforms were shown to have major impact on TSSA antigenicity, leading to negligible cross-reactivity between them [21]. This property was proposed to have great epidemiological value, as it allowed for typification of the infecting strain by simple serological methods. Recent studies challenged this idea by showing that TSSA is significantly more diverse in amino acid structure than described previously [22], although the antigenic impact of these variations, if any, remains uncertain. In the present study, we investigated the possible role(s) of TSSA on T. cruzi attachment to and internalization into mammalian cells by carrying out comparative biochemical and genetic studies of TSSA isoforms from parasite extant evolutionary lineages.

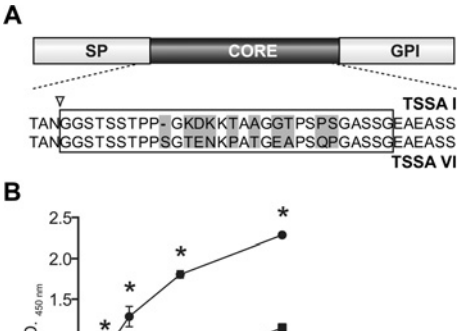
#### **EXPERIMENTAL**

## Parasite stocks and cell lines

CL Brener and Sylvio X-10 stocks were used as representatives of TcVI and TcI evolutionary lineages respectively. Epimastigotes were grown at 28 °C in brain/heart/tryptose medium supplemented with 10 % (v/v) heat-inactivated FBS (fetal bovine serum). Cell-derived trypomastigote and amastigote forms were harvested from the supernatant of *Mycoplasma*-free Vero-infected cells grown in MEM (minimal essential medium) [23]. Cell lines were from the A.T.C.C. (Manassas, VA, U.S.A.) and were grown at 37 °C in 5 % CO<sub>2</sub> in the indicated medium supplemented with 10 % (v/v) FBS, 0.292 g/l L-glutamine, 100 IU/ml penicillin and 100  $\mu$ g/ml streptomycin (all from Gibco Laboratories) unless stated otherwise.

## **Recombinant proteins**

Genes coding for Sylvio X-10 TSSA (TSSA I) and CL Brener TSSA (TSSA VI) have been described previously [22,24]. GST (glutathione transferase)-fusion proteins consisted only of the



2.5 2.0 2.0 2.0 2.0 3 1.0 0.5 0 1.0 0 50 100 protein concentration (μg/ml)

Figure 1 TSSA binding to non-phagocytic cells

(A) Schematic representation and alignment of TSSA I and TSSA VI sequences used as GST-fusion molecules. Variable positions are shaded. Sequences included in tssa I/VI peptides are boxed. The predicted SP cleavage site is indicated with a triangle. GPI, glycosylphosphatidylinositol-anchoring signal. (B) Increasing amounts of GST ( $\blacksquare$ ), GST–TSSA I ( $\triangle$ ) or GST–TSSA VI ( $\bullet$ ) were added to Vero cells and binding was assessed by means of anti-GST Abs followed by a colorimetric method. O.D.  $_{450 \text{ nm}} = D_{450}$ . Results are means  $\pm$  S.D. for three independent experiments performed in triplicate. \* $^{*}P$  < 0.005 compared with GST values using Student's  $^{t}$  test.

predicted full-length mature products, i.e. without most of the SP (signal peptide) and the GPI-anchoring signal (Figure 1A). Supernatants of *Escherichia coli* strain BL21(DE3) cultures induced for 3 h at 28 °C with 0.1 mM isopropyl  $\beta$ -D-thiogalactopyranoside (Fermentas) were purified by gluthatione–Sepharose chromatography (GE Healthcare) and dialysed against PBS. GST–TSSA samples were quantified using the Bradford reagent (Pierce) and purity was assessed by silver staining after SDS/PAGE [24].

## Synthetic peptides

Peptides were custom-synthesized (Sigma-Genosys) bearing an additional cysteine residue (in italics) at their C-termini. Sequences were: GGSTSSTPPSGTENKPATGEAPSQPGASSGC (tssa VI), GGSTSSTPPGTDKKTAAGGTPSPSGASSGC (tssa I) and AVFKAAGGDPKKNTTC (smug L).

## Ca2+ dynamics assay

HEK (human embryonic kidney)-293 cells (3×10<sup>4</sup>) grown in DMEM (Dulbecco's modified Eagle's medium) were seeded on black-wall clear-bottom 96-well plates (Costar). After 24 h of incubation, cells were loaded with Fluo-4 (Invitrogen) at 5 μM in DMEM (40 μl/well) [25]. After 1 h of incubation, medium was replaced by 190 μl/well HBSS (Hanks balanced salt solution: 5.4 mM KCl, 0.3 mM Na<sub>2</sub>HPO<sub>4</sub>, 0.4 mM KH<sub>2</sub>PO<sub>4</sub>, 4.2 mM NaHCO<sub>3</sub>, 0.5 mM MgCl<sub>2</sub>, 0.6 mM MgSO<sub>4</sub>, 5.6 mM Dglucose, 136.8 mM NaCl and 2 mM CaCl<sub>2</sub>). Plates were read for 275 s in a Flexstation 3 plate fluorimeter (Molecular Devices), and peptides, dissolved in HBSS, were added at 50 s. Fluo-4 was excited at 488 nm, and emitted fluorescence was selected with a 515 nm cut-off filter and a 515 nm emission filter.

## ERK (extracellular-signal-regulated kinase) 1/2 analysis

HeLa cells grown in DMEM were serum-starved for 12 h before treatment with 10 ng/ml recombinant hEGF (human endothelial growth factor) (Invitrogen) with the indicated peptide dissolved in high-glucose DMEM. A range of peptide concentrations (10–500 nM) and pre-incubation times (0–30 min) were evaluated previously (not shown), and maximal effects were recorded at 50 nM and 5 min respectively. After hEGF treatment, cells were rinsed in ice-cold PBS, lysed in Laemmli buffer, and analysed by Western blotting using anti-ERK2 (sc-154) or anti-phospho-ERK1/2 (sc-7383) Abs (1:1000 dilution) followed by HRP (horseradish peroxidase)-conjugated secondary Abs (all from Santa Cruz Biotechnology). Immunoreactive bands were visualized with the Immobilon Western Chemiluminescent HRP Substrate (Millipore), and densitometric analyses were carried out using ImageJ (NIH).

#### Binding of TSSA to cell monolayers

HeLa or Vero cells  $(5\times10^4)$  placed in 96-well culture plates were grown overnight in DMEM or MEM respectively, fixed with PBS containing 4% (w/v) paraformaldehyde for 10 min, blocked with PBS containing 10% (v/v) FBS for 1 h, and incubated with the indicated GST-fusion protein for 1 h followed by rabbit GST antiserum or anti-GST (GST-2, Sigma) mAb (monoclonal Ab), both diluted 1:1000 in PBS containing 2% (v/v) FBS. Plates were washed with PBS (four times, 5 min each), before the corresponding HRP-conjugated secondary Abs were added at a dilution of 1:5000 in PBS containing 2% (v/v) FBS followed by  $100~\mu l$  of 3,3',5,5'-tetramethylbenzidine (Sigma) and  $100~\mu l$  of 2 M sulfuric acid, and read at 450 nm.

## Purification of anti-(TSSA VI) antibodies

Purified GST-TSSA VI protein (2 mg) was immobilized on to a *N*-hydroxysuccinimide-activated column (HiTrap<sup>®</sup>, GE Healthcare) [23]. Anti-(TSSA VI) Abs were purified from the serum of a GST-TSSA-VI-immunized rabbit [21] by affinity chromatography [23].

#### Attachment/infection assays

HeLa or Vero cells  $(5\times10^4)$  grown on 24-well culture plates in DMEM or MEM respectively were added with  $5\times10^5$  cellderived trypomastigote forms (when indicated, containing 25 % extracellular amastigotes) in the presence of the indicated peptide. After 3 h of incubation at 37 °C, cells were washed with PBS and fixed with PBS containing 4% (w/v) paraformaldehyde either immediately (attachment/internalization assays) or after an additional 36 h of incubation in MEM containing 4 % (v/v) FBS (infection assays). Following extensive washing in PBS, cells were incubated for 10 min with 25 mM NH<sub>4</sub>Cl and blocked for 1 h in PBS containing 2% (w/v) BSA and 2% (v/v) normal goat serum. Extracellular (attached) parasites were labelled with the addition of a T. cruzi-infected mouse serum (1:500 dilution in blocking buffer) followed by Alexa Fluor® 488-conjugated secondary Abs (Molecular Probes, diluted 1:1000 in blocking buffer). Intracellular parasites were subsequently labelled with the addition of a T. cruzi-infected rabbit serum (1:500 dilution in blocking buffer with 0.5% saponin) followed by Alexa Fluor® 564-conjugated secondary Abs (Molecular Probes, diluted 1:1000 in blocking buffer). Slides were mounted with 10  $\mu$ l of Fluor Save reagent (Calbiochem) containing 1 μg/ml DAPI (4',6diamidino-2-phenylindole) (Invitrogen) and analysed in a Nikon Eclipse E600 microscope coupled to a SPOT RT<sup>TM</sup> colour camera (Diagnostic Instruments). The infection rate was determined by manual counting of infected and non-infected cells using the ImageJ plug-ins Cell Counter and Nucleus Counter in at least 1000 DAPI-stained cells. For attachment/internalization assays, every cell-associated parasite including (i) recently internalized parasites, (ii) parasites caught in the process of invasion, and (iii) extracellular parasites attached to the cell surface, was considered and manually counted in at least 1000 DAPI-stained cells. To assay the effect of Abs, parasites were incubated for 30 min with purified Abs diluted in PBS before addition to cell cultures.

#### Parasite transfection and analysis

Genomic DNA from Sylvio X-10 or CL Brener stocks [21] was used as the template for two independent PCRs with oligonucleotides TSSA<sub>Fw</sub> and either TSSAI<sub>Rev</sub> or TSSAVI<sub>Rev</sub> (SPcore constructs), and GPITSSA<sub>Fw</sub> and GPITSSA<sub>Rev</sub> (common GPI construct) (Supplementary Table S1 at http://www.BiochemJ. org/bj/444/bj4440211add.htm). Amplification products were purified and cloned into pGEM-T easy vector (Promega). The GPI construct was digested with EcoRI/HindIII (Fermentas) and cloned into the trypanosomatid expression vector pTREX omni yielding pTREX omni GPI. Both SP-core constructs were digested with XbaI/ClaI and separately ligated into pTREX omni GPI, thus yielding the FLAG-tagged TSSA I and TSSA VI fulllength constructs. pTREX omni was generated by insertion of an XbaI/XhoI cassette bearing multiple cloning sites and a FLAG tag from pDIY-eG vector (GenBank® accession number JN596089) into the pTREXL-Neo vector (GenBank® accession number JN596094) (L. A. Bouvier, M. M. Cámara, G. E. Cánepa, M. M. Miranda and C. A. Pereira, unpublished work). Epimastigotes (1.5×108) from the Adriana stock (TcI) were electroporated, selected with 200  $\mu$ g/ml G418 (Gibco Laboratories), and used as populations at least 45 days afterwards [26]. For flow cytometry analysis, parasites were washed, blocked in PBS containing 10% (v/v) FBS, and incubated with anti-FLAG M2 mAb (Sigma, 1:500 dilution) in an ice-water bath followed by Alexa Fluor® 488-conjugated secondary Abs. After several washes, parasites were resuspended in 300 µl of PBS containing 4% (w/v) paraformaldehyde and analysed using FACS CyFLOW Partec and FloMax software. IFAs (indirect immunofluorescence assays) were carried out as described in [23,26]. GPI-anchored proteins were purified following the protocol described in [27]. Briefly,  $1.5 \times 10^8$  parasites were homogenized in 2 ml of GPI buffer [10 mM Tris/HCl (pH 7.4), 150 mM NaCl, 2% Triton X-114, 1 mM PMSF and a protease inhibitor cocktail (Sigma)] on ice for 1 h and centrifuged at 8800 g for 10 min at 0 °C. The supernatant was stored at -20 °C for 24 h, thawed, homogenized and submitted to phase separation at 37 °C for 10 min followed by centrifugation at 3000 g for 3 min at room temperature (25 °C). The upper aqueous phase was discarded and the lower detergentrich phase was added to 1 ml of buffer A (10 mM Tris/HCl, pH 7.4, 150 mM NaCl, 0.06 % Triton X-114 and 1 mM PMSF), incubated at 0°C for 10 min, and submitted to a new phase separation as above. The detergent-rich phase was added to 1 ml of buffer A, homogenized, incubated for 30 min at 0°C and centrifuged at 18 000 g for 10 min at 0 °C. The supernatant (S4) was submitted to a new phase separation, and the detergent-rich phase was taken as the GPI fraction. Aliquots of the S4 fractions were precipitated with ice-cold acetone, resuspended in 200  $\mu$ l of 10 mM Tris/HCl (pH 7.2), 0.1 % sodium deoxycholate and treated for 3 h with 0.3 unit of PI-PLC (phosphatidylinositolspecific phospholipase C) from Bacillus cereus (Invitrogen) at 37 °C. Samples were then re-precipitated, resuspended in 200  $\mu$ l of GPI buffer, and submitted to phase separation. Both phases were analysed by Western blotting with anti-FLAG mAb (1:5000 dilution) [26]. To purify mucins, 109 parasites were delipidated by water/chloroform/butan-1-ol treatment (0.8:1:2, by vol.) [28]. The butan-1-ol phase (F1) contains mainly phospho- and glyco-lipids, whereas the aqueous phase (F2) is enriched in mucintype glycoproteins. Delipidated parasites were also extracted with 9% butan-1-ol in water and the mucin-rich aqueous phase (F3) was extracted further with 91% butan-1-ol (F4). Final parasite pellets (P) were resuspended in Laemmli buffer containing 6 M urea and 100  $\mu$ g/ml DNase I (Sigma). Fractions were analysed by Western blotting as above. Attachment of epimastigotes was performed and evaluated as described for cell-derived trypomastigote forms except that (i)  $5 \times 10^6$  parasites were seeded on to  $5 \times 10^4$  Vero cells, and (ii) no intracellular parasites were detected.

## RT (reverse transcription)-PCR and cDNA analysis

Total RNA was extracted from  $2\times10^8$  Sylvio X-10 cell-derived trypomastigote forms with TRIzol® reagent and cDNA synthesized using SuperScript II (Invitrogen) [26]. TSSA I 5′-UTR (untranslated region) was amplified by PCR using oligonucleotides mini-exon and TSSAI<sub>Rev</sub>, and TSSA I 3′-UTR using oligonucleotides TSSAI<sub>Fw</sub> and Oligo(dT) anchor (Supplementary Table S1). Final amplification products were cloned into pGEM-T easy and sequenced. The complete TSSA I cDNA (GenBank® accession number JQ354939) is a composite of these two sequences.

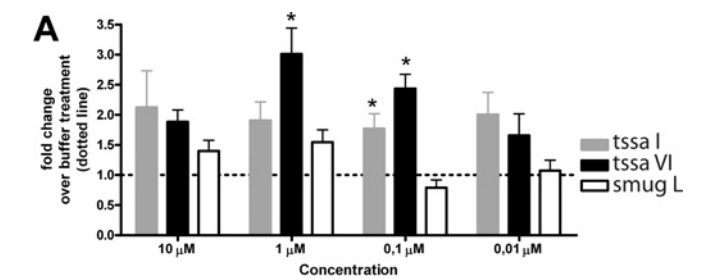
#### **RESULTS**

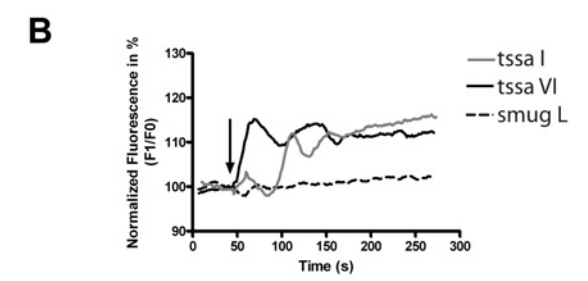
#### Binding of TSSA molecules to mammalian cells

As a first step towards functional evaluation of TSSA, we developed an adhesion assay in which microplates containing paraformaldehyde-fixed HeLa cells were incubated with increasing amounts (12.5-100 µg/ml) of GST-TSSA proteins (Figure 1A), and molecules retained were detected by anti-GST polyclonal Abs. As shown in Figure 1(B), GST-TSSA VI binding to HeLa cells was dose-dependent and saturable, indicating a possible ligand-receptor interaction. A GST control tested in parallel yielded significantly lower attenuance values within the protein range tested. Interestingly, GST-TSSA I showed negligible binding to HeLa cells, thus indicating that minor sequence variation between TSSA isoforms have a great impact in terms of their adhesion properties. Quite similar results were obtained when binding assays were carried out using paraformaldehyde-fixed Vero cells and/or revealed with a commercial mAb against GST (results not shown).

## TSSA signalling in mammalian cells

In addition to mediating parasite-host cell interaction, different T. cruzi adhesins trigger signalling pathways in the target cell. Induction of Ca<sup>2+</sup> fluxes in the host cell is of particular interest, as it was shown to promote parasite invasion directly [10]. To determine whether TSSA isoforms had Ca<sup>2+</sup>-mobilization properties, we measured Ca2+ dynamics in HEK-293 cells preloaded with a fluorescent Ca<sup>2+</sup> indicator. As shown in Figure 2(A), HEK-293 cells mobilized Ca<sup>2+</sup> to the cytoplasm in a sustained manner upon addition of a synthetic peptide spanning most of the predicted mature region of either TSSA VI (tssa VI) or TSSA I (tssa I). Responses of tssa I and tssa VI were consistently higher than those elicited by a control peptide derived from the epimastigote-restricted mucin TcSMUG L [26]. In particular, statistical significance compared with the smug L peptide was observed at 1  $\mu$ M and 0.1  $\mu$ M for tssa VI and at 0.1  $\mu$ M for tssa I. Although both TSSA-derived peptides showed roughly similar end-point effects, differences between them became evident when analysing the kinetics of the induced Ca<sup>2+</sup> responses. As shown in





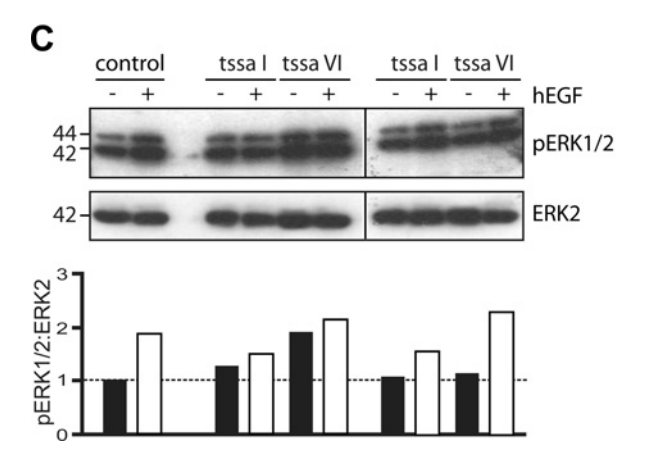


Figure 2 TSSA signalling in non-phagocytic cells

(A) Ca<sup>2+</sup> response induced in HEK-293 cells by addition of increasing amounts of tssa I (grey bars), tssa VI (black bars) or smug L (white bars) peptide. Results were normalized to the responses obtained by the addition of buffer (broken line) and the response was calculated as the difference between maximum and minimum Fluo-4 emitted fluorescence. Results are means + S.D. for three experiments. Data were analysed separately for each peptide  $concentration\,using\,Graph Pad\,Software.\,{}^\star P < 0.05\,compared\,with\,corresponding\,smug\,L\,values$ using Newman-Keuls post-test analysis. (B) Representative time series graphics obtained upon addition (arrow) of 0.1  $\mu$ M tssa I (grey line), tssa VI (black line) or smug L (broken line) peptide. Fluorescence was normalized to the baseline by obtaining the mean of the first ten fluorescence points in each graph (named F0), dividing each point of fluorescence in the graph (named F1) by F0 and multiplying by 100. (C) HeLa cells were serum-starved for 12 h before addition of high-glucose DMEM (control) or the indicated peptide (50 nM). hEGF (10 ng/ml) was added or not to cells pre-treated with the indicated stimulus for 5 min (left-hand panels) or 15 min (right-hand panels). Cells were lysed 5 min afterwards and processed for Western blotting against phospho-ERK1/2 (upper panels) and ERK2 (lower panels). Molecular markers (in kDa) are indicated. Ratio of phosphoERK1/2 to ERK2 of cells with (white bars) or without (black bars) hEGF is shown in the histogram.

Figure 2(B), projections of the entire time series upon addition of 100 nM of either peptide, i.e. the concentration yielding maximal differences between tssa I/VI and smug L as determined in Figure 2(A), indicated that tssa VI elicited a much more rapid and sustained increase in intracellular Ca<sup>2+</sup> compared with tssa I, suggesting that they have different affinities/modes of action.

Ca<sup>2+</sup> has been implicated as a potential regulator of different MAPK downstream effectors, including the ERK1/2 cascade

[29,30]. Indeed, up-regulation of ERK1/2 phosphorylation, which probably exerts an anti-apoptotic effect on target cells, is a diagnostic feature following invasion of cell-derived trypomastigote forms [8,31]. We therefore examined the effect of TSSA-derived peptides on basal and hEGF-stimulated ERK1/2 phosphorylation in a non-phagocytic cell model (HeLa cells). Control HeLa cultures maintained under serum-starved conditions showed strong ERK1/2 phosphorylation (1.89-fold) upon addition of hEGF (Figure 2C). Pre-incubation of cells for 5 min with 50 nM tssa I did not have a clear effect, as it slightly increased (1.3-fold) the basal HeLa response, but decreased the hEGF-induced ERK1/2 phosphorylation (from 1.89- to 1.52-fold). In stark contrast, preincubation of cells for 5 min with 50 nM tssa VI functioned as a potent stimulator for this pathway, inducing a robust up-regulation of ERK1/2 phosphorylation (1.93-fold). Addition of hEGF led to a modest ERK1/2 phosphorylation stimulation in tssa VI-treated cells, suggesting that hEGF and tssa VI activate (at least partially) converging signalling pathways. The effect verified for tssa VI was transient, as demonstrated using a similar experimental setup following 15 min of pre-incubation with the peptide. Together with the Ca<sup>2+</sup> dynamics results shown above, these findings indicate that TSSA in the range 50-100 nM displays isoformspecific signalling properties over mammalian cells.

# TSSA is involved in host cell infection by cell-derived trypomastigotes

We next examined whether TSSA recognition/sensitization of the host cell had a functional correlate in terms of parasite infection. To that end, we resuspended CL Brener cell-derived trypomastigote forms (which express TSSA VI) in PBS supplemented with increasing amounts of the indicated GST-fusion protein, and seeded them on top of Vero cell monolayers. The infection rate was determined 39 h afterwards by direct counting of infected and non-infected cells, and found to be inhibited in a dose-dependent manner by the addition of GST-TSSA VI (results not shown). At 200  $\mu$ g/ml, Vero cell infection was impaired up to 34 % compared with a control GST molecule (Figure 3A), although variations between experiments precluded statistical significance. In line with binding data, addition of GST-TSSA I had consistently minor and non-significant effect on the infectivity of CL Brener cell-derived trypomastigote forms.

We next assayed the inhibitory capacity of peptides tssa I and VI in similar infection assays. Briefly, tssa VI spanning the central core of TSSA VI (Figure 1A) had a significant inhibitory effect on CL Brener cell-derived trypomastigotes infectivity in both Vero and HeLa cells, whereas tssa I peptide had a negligible effect on this process (Figure 3B). As in the case of GST-fusion proteins, no effect of tssa peptides on cell and/or parasite viability, as evaluated by motility and Trypan Blue exclusion, was observed (results not shown). Representative low-magnification images highlighting differences in parasite burden in Vero cells upon addition of either peptide are shown in Supplementary Figure S1 (http://www.BiochemJ.org/bj/444/bj4440211add.htm). Quite similar results were obtained upon pre-incubation of CL Brener cell-derived trypomastigote forms with increasing amounts of purified Abs before infection assays. As shown in Figure 3(C), anti-TSSA VI Abs inhibited cell-derived trypomastigote infection in a dose-dependent manner. At the maximal concentration tested (100 μg/ml), anti-TSSA VI Abs significantly decreased infectivity of CL Brener cell-derived trypomastigote forms by  $\sim$  85 % compared with pre-immune IgG.

We then carried out short-term (3 h) assays in the presence of exogenously added peptides. In contrast with long-term (39 h) assays described above, every cell-associated parasite,

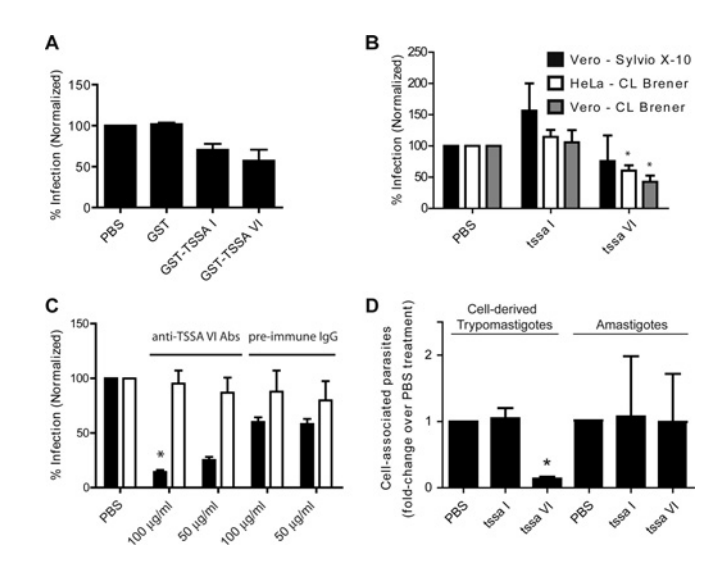


Figure 3 TSSA is involved in parasite internalization

(A) Infection rate of CL Brener cell-derived trypomastigate forms on Vero cell monolayers in the presence of 200  $\mu$ g/ml of the indicated GST-fusion protein or PBS. (**B**) Infection rate using different cell-derived trypomastigotes stock-cell line combinations (CL Brener-HeLa, white bars; CL Brener-Vero, grey bars; Sylvio X-10-Vero, black bars) in the presence of 500  $\mu$ g/ml of the indicated peptide or PBS. (C) Infection rate of CL Brener (black bars) or Sylvio X-10 (white bars) cell-derived trypomastigote forms that were pre-incubated with anti-TSSA VI Abs or pre-immune IgG before incubation with Vero cell monolayers. In (A)–(C), the number of infected cells was determined in a total of at least 1000 DAPI-stained cells and normalized to control (PBS) values, which varied within the range of 18–32 infected cells/100 cells. Results are means  $\pm$  S.D. for three (four in **A**) independent experiments performed in duplicate.  ${}^{\star}P < 0.05$  compared with the corresponding control (PBS in A and B, pre-immune IgG in C) values using Student's t test. (D) A mixture of CL Brener parasites (75% cell-derived trypomastigote forms, 25% extracellular amastigote forms) were seeded on top of Vero cell monolayers in the presence of PBS, tssa I or tssa VI peptide. The number of either cell-associated parasite form (as defined in the Experimental section) in a total of at least 1000 DAPI-stained cells was determined 3 h afterwards and normalized to control (PBS) values, which varied within the range of 18-42 cell-derived trypomastigotes/100 cells and 6–12 amastigotes/100 cells respectively. Results are means + S.D. for three independent experiments performed in duplicate. \*P < 0.05 compared with the corresponding control (PBS) values using Student's t test.

i.e. those extracellular (although firmly attached to the cell surface), recently internalized or caught in the invasion process, was considered and counted. As shown in Figure 3(D), attachment/internalization of cell-derived trypomastigote forms was significantly impaired (>80% inhibition) in the presence of tssa VI peptide. Interestingly, attachment/internalization of amastigote forms present in the parasite inocula was not significantly affected by the addition of either peptide, which is compatible with their lack of TSSA expression [21] (Supplementary Figure S2 at http://www.BiochemJ.org/bj/444/ bj4440211add.htm). Together, these findings indicate that TSSA VI is specifically involved in CL Brener cell-derived trypomastigote infection of different non-phagocytic cell lines. Since similar inhibitory effects were obtained in short- and longterm assays, it is likely that the TSSA VI main contribution to cell-derived trypomastigote infectivity is exerted during the attachment phase rather than during the intracellular growth.

To evaluate further the role of TSSA in *T. cruzi* infection, we carried out cell-infection assays using Sylvio X-10 cell-derived trypomastigote forms (which bear a *TSSA I* gene). Pre-incubation with anti-TSSA VI Abs, which did not label Sylvio X-10 parasites by IFA or Western blotting (Supplementary Figure S2), did not inhibit infectivity of Sylvio X-10 cell-derived trypomastigote forms (Figure 3C). In the same line, addition of tssa VI had no significant effect on this experimental set-up, supporting further the specificity of the above results (Figure 3B).

Unexpectedly, these assays also indicated that the tssa I peptide had no effect on the infectivity of Sylvio X-10 cell-derived trypomastigote forms, suggesting that TSSA I, in contrast with TSSA VI, is not involved in parasite attachment/internalization. To address this issue, we sought to obtain insights into the expression of TSSA I. RT-PCR assays allowed us to isolate and characterize the specific mRNA from Sylvio X-10 cell-derived trypomastigote forms (Supplementary Figure S3 at http://www.BiochemJ.org/bj/444/bj4440211add.htm). TSSA I mRNA is highly similar to the CL Brener one, and completely processed by trans-splicing and polyA addition, strongly suggesting a genetically active state of the TSSA locus in this parasite form. TSSA I antisera, however, did not reveal immunoreactive bands in lysates prepared from different developmental forms of Sylvio X-10 or other TcI/TcVI parasite stocks following Western blot analyses (Supplementary Figure S2 and results not shown). It should be stated that TSSA I antisera raised using different combinations of immunogens, adjuvants and/or animal species presented consistently very poor affinity/titre, thus compromising the sensitivity of these analyses.

# Transfected epimastigotes overexpressing TSSA interact with host cells

TSSA belongs to a complex family of mucin-type genes distributed throughout the T. cruzi genome. This, along with the underdeveloped genetic tools in this parasite, makes it impractical for a knockout/knockdown approach. To circumvent this hurdle, we attempted a functional complementation strategy [32]. To that end, epimastigotes, i.e. the non-infective parasite form found in the insect midgut, of the Adriana stock (TcI) were stably transfected with a T. cruzi expression vector carrying a FLAG-tagged version of either TSSA VI or TSSA I cDNA [26]. Transfected epimastigote populations, along with appropriate controls, were incubated with Vero cells for 3 h, and the attachment rate was determined as above. In line with binding data, epimastigotes overexpressing CL Brener TSSA exhibited a significant ( $\sim$ 2-fold) increase in their adhesion properties compared with those overexpressing the Sylvio X-10 counterpart (Figure 4A).

Western blot analyses revealed similar expression rates for both transgenic TSSA molecules, which migrated in nonreducing SDS/PAGE as broad  $\sim 20 \text{ kDa}$  species (Figure 4B). This apparent molecular mass is similar to that verified for the CL Brener cell-derived trypomastigote-expressed product ( $\sim 15 \text{ kDa}$ , Supplementary Figure S2). Following Triton X-114 fractionation assays, both molecules were highly concentrated in the final detergent phase, thus indicating that they are indeed GPI-anchored proteins (Figure 4C). Moreover, transgenic TSSA molecules were readily 'solubilized' (although without concomitant recovery in the aqueous phase), upon PI-PLC treatment (Figure 4C), hence supporting (i) their anchorage to the outer layer of the plasma membrane through a GPI lipid motif, and (ii) their mucin-type nature [26] (see below). IFA- and flow cytometry-based results argue further for membrane localization of both TSSA products (Figure 4D and results not shown). Interestingly, transgenic TSSA I and TSSA VI showed a punctate pattern over the periphery of the entire parasite body and, although to a much lesser degree, the flagellum, which is very reminiscent of the distribution of the endogenous TSSA protein expressed by cellderived trypomastigotes (Supplementary Figure S2). To continue our analysis on the post-translational processing of transgenic molecules, total mucin-type species were purified from both TSSA I- and TSSA VI-transfected populations following a standard butan-1-ol extraction protocol [28], and aliquots from different

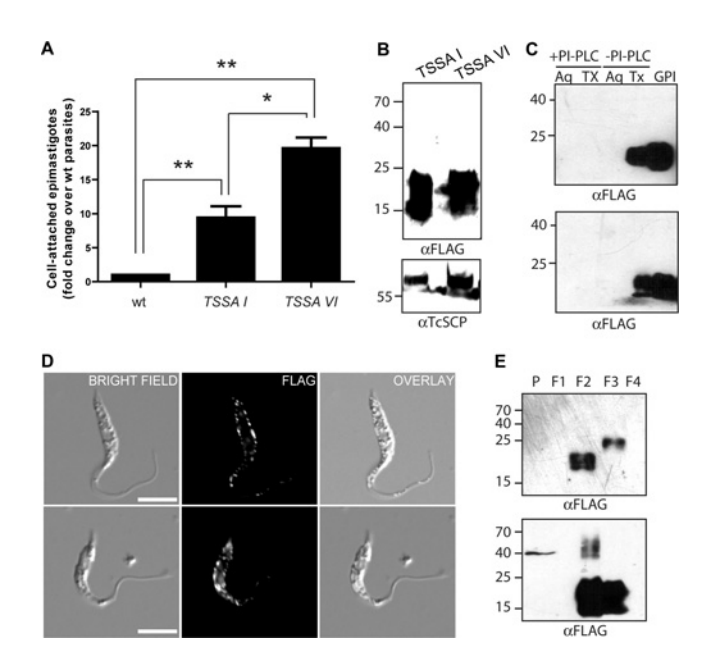


Figure 4 Expression and biochemical analyses of TSSA products in transgenic epimastigotes

(A) Epimastigotes transfected with TSSA I or TSSA VI or non-transfected (wt) were seeded on top of Vero cell monolayers and the attachment rate was determined 3 h later in a total of at least 1000 DAPI-stained cells and normalized to control (wt) values. Results are means + S.D. for three independent experiments performed in duplicate. \*P < 0.05, \*\*P < 0.005 using Student's t test. (B) Total lysates from epimastigotes transfected with TSSA I or TSSA VI were probed either with anti-FLAG mAb (upper panel) or serine carboxypeptidase (TcSCP) antiserum (1:3000 dilution, lower panel) [26]. Molecular masses are indicated in kDa. (C) Equal amounts of epimastigotes transfected with TSSA I (upper panel) or TSSA VI (lower panel) were fractionated with Triton X-114 (see the Experimental section) and equivalent samples from the final detergent-rich fractions (GPI) were probed with anti-FLAG mAb. In addition, aliquots of the S4 fractions were treated or not with PI-PLC and re-partitioned using Triton X-114 and the detergent-rich (TX) and aqueous (Aq) phases were probed with mAb anti-FLAG. Molecular masses are indicated in kDa. (**D**) IFA of non-permeabilized epimastigotes transfected with TSSA I (lower panels) or TSSA VI (upper panels) revealed with anti-FLAG mAb. No FLAG signal was detected in non-transfected epimastigotes (not shown). Scale bars, 10  $\mu$ m. (**E**) Butan-1-ol extraction analysis of epimastigote populations transfected with TSSA I (upper panel) or TSSA VI (lower panel). Fractions (see the Experimental section) were resolved by SDS/PAGE (15 % gels) and probed with anti-FLAG mAb. Molecular masses are indicated in kDa.

fractions were probed by Western blotting using an anti-FLAG mAb. As shown in Figure 4(E), in both cases, FLAG reactivity was restricted to F2 and F3 fractions, thus coincident with the fractionation pattern of endogenous epimastigote mucins [26,28]. In the case of TSSA VI-transfected parasites, minor ~40–55 kDa products, which probably constitute TSSA aggregates, could be observed in the F2 and pellet fractions. Taken together, these findings indicate that, in spite of TSSA I and TSSA VI products being processed as mucin-type molecules and properly displayed in approximately equivalent amounts on the surface of transfected epimastigote forms, TSSA VI provides a significantly better adhesion molecule for parasite recognition of the target cell.

## **DISCUSSION**

TSSA shows substantial structural homology with members of the *T. cruzi* family of mucin-type genes, particularly with those belonging to the *TcMUC* group, which are also expressed by the mammal-dwelling stages of the parasite [17,23,33]. Biochemical analyses of the endogenous cell-derived trypomastigote-expressed product [21], as well as the recombinant products expressed by transfected epimastigotes, indicate that

TSSA is indeed processed and displayed on the parasite surface as a mucin-type molecule. However, in contrast with most T. cruzi mucin-type proteins [17,23], TSSA does not seem to undergo extensive O-glycosylation in vivo. On one hand, TSSA migrates in non-reducing SDS/PAGE as a  $\sim 15-20$  kDa species, thus well below the molecular mass determined for epimastigote mucins ( $\sim$ 35–50 kDa) bearing similar scaffolding polypeptides [26]. On the other hand, synthetic peptides and/or recombinant proteins spanning linear B-cell antigenic determinants of the TSSA central region, i.e. the only one exposed on the parasite surface upon processing of the SP and GPI-anchoring signal, are strongly recognized by sera from most Chagasic patients and T. cruzi-infected animals [21,24,34]. Moreover, Abs raised against TSSA molecules expressed in bacteria, thus lacking glycosylation, readily label TSSA on the surface of cell-derived trypomastigote forms. These features indicate the exposition of 'naked' (i.e. non-glycosylated) peptide sequences on cell-derived trypomastigote-displayed TSSA molecules, and uphold the use of recombinant proteins and synthetic peptides as appropriate tools for the evaluation of TSSA functional properties.

As shown, binding of epimastigote forms to non-macrophagic cells is increased ~2-fold upon transfection with CL Brener TSSA compared with those transfected with Sylvio X-10 TSSA. Moreover, recombinant TSSA VI binding to different types of cells is dose-dependent and saturable, indicating a likely interaction with protein receptor(s). Accordingly, addition of tssa VI peptide or anti-TSSA VI Abs inhibits both attachment and infectivity of CL Brener cell-derived trypomastigote forms by up to 85%. These findings suggest that TSSA VI is part of the repertoire of surface molecules orchestrating cell-derived trypomastigote invasion of the target cell. According to current knowledge, parasite surface adhesins can function either as up-regulators or down-regulators of cell-derived trypomastigote invasion, i.e. molecules that trigger an inhibitory pathway in the target cell, thus leading to a net negative impact on parasite infectivity as proposed for metacyclic trypomastigote-restricted gp90 [7]. Our data are compatible with TSSA VI belonging to the former class, and contributing both to parasite attachment to and downstream signalling in the target cell. Accordingly, we envisage a model in which TSSA VI engagement to an as-yet-undefined receptor(s) displayed on the surface of nonmacrophagic mammalian cell contribute in providing the parasite with a solid grasp before its effective internalization. Addition of soluble tssa VI or specific Abs has a detrimental effect on parasite infectivity by interfering with or directly blocking this ligandreceptor pairing. Even though tssa VI triggers Ca<sup>2+</sup> mobilization and ERK1/2-based signalling cascades in the host cell, the fact that addition of exogenous peptide does not significantly affect Sylvio X-10 cell-derived trypomastigote infectivity suggests a minor role for TSSA downstream signalling in parasite infectivity.

We reported previously that sequence variations between TSSA isoforms have a major impact on their antigenicity [21,24]. In the present study, we have shown that these differences also have a functional correlate in terms of TSSA adhesion/signal transduction properties. The molecular basis underlying these contrasting effects is not yet understood, although it is unlikely that site-specific and mostly conservative changes observed in TSSA I will overhaul the overall three-dimensional structure of this molecule. In line with the above-mentioned model, we speculate that these subtle changes impair recognition of specific binder(s) on the target cell by TSSA I. Molecular identification and functional characterization of TSSA VI host cell receptor(s) will be instrumental to address this issue and is currently underway.

Quite oddly, addition of soluble tssa I does not affect in vitro infectivity of Sylvio X-10 cell-derived trypomastigote forms. Two possibilities can be envisaged to explain this finding: on one hand, TSSA I is not translated at detectable levels in TcI cell-derived trypomastigote forms due to posttranscriptional regulation mechanisms acting on its mRNA. This is a rather common theme in T. cruzi expression regulation [35], and we indeed identified a putative destabilizing-like structure in the 3'-UTR of the Sylvio X-10 mRNA [36] (Supplementary Figure S3). Alternatively, TSSA I might indeed be translated in Sylvio X-10 cell-derived trypomastigote forms, but subjected to post-translational processing to prevent its recognition by Abs raised against peptide epitopes. Whatever the case, and in contrast with CL Brener cell-derived trypomastigotes, target cell recognition/invasion capabilities of Sylvio X-10 trypomastigotes are not likely to be associated with the peptide scaffolding of TSSA. Quantitative and/or qualitative differences in the function/expression of components of the metacyclic trypomastigote surface coat among parasite isolates belonging to distinct evolutionary lineages have been reported previously [7,19]. When it comes to cell-derived trypomastigote forms, only variations in surface-associated TS activity were shown so far to correlate with differences in parasite infectivity and virulence [37]. As reported, TcVI isolates, which lead to uncontrolled parasitaemia and 100 % mortality in infected mice, show significantly increased TS expression/secretion compared with TcI stocks, which lead to mild and transient lesions and 100% chronicity upon injection into mice littermates. Likewise, TcVI parasite stocks were reported to display increased virulence and parasitaemia in T. cruzi-infected individuals compared with TcI stocks [38,39]. The results of the present study showing that antigenic and adhesive TSSA isoforms are present in TcVI parasite stocks, but not in TcI ones, fit snugly within this theoretical framework.

In summary, we have shown that TSSA plays an important role in *T. cruzi* infectivity. Since there are no homologues of *TSSA* in related protozoa or vertebrates, this gene and its encoded protein could be excellent targets for molecular intervention in Chagas' disease. Furthermore, the facts that TSSA is highly immunogenic, abundantly expressed on the parasite surface and that Abs raised against TSSA neutralize *T. cruzi* infection of non-macrophagic cells suggest that TSSA could also be a candidate for vaccine development.

#### **AUTHOR CONTRIBUTION**

Gaspar Cánepa, Celia Garcia and Carlos Buscaglia conceived and designed the experiments. Gaspar Cánepa, Maria Sol Degese and Alexandre Budu performed the experiments. Gaspar Cánepa, Maria Sol Degese, Alexandre Budu, Celia Garcia and Carlos Buscaglia analysed the data. Gaspar Cánepa and Carlos Buscaglia wrote the paper.

## **ACKNOWLEDGEMENTS**

We thank Oscar Campetella (IIB-INTECh) and Susana Leguizamón (University of Buenos Aires) for tssa peptides, León Bouvier and Claudio Pereira (Instituto de Investigaciones Médicas Alfredo Lanari, Buenos Aires) for the pTREX omni vector, Daniel Sánchez and Valeria Tekiel (IIB-INTECh) for the sera of T. cruzi-infected rabbits and mice, and Alejandro Cassola (IIB-INTECh), Juan Cazzulo (IIB-INTECh) and Omar Coso (IFIBYNE) for kindly providing reagents. We are also indebted to Agustina Chidichimo and Liliana Sferco for culturing parasites.

## **FUNDING**

G.E.C. and M.S.D. hold fellowships from the Argentinean Research Council (CONICET), and C.A.B. is a career investigator from the same institution. This work was supported by the Fundação de Amparo à Pesquisa do Estado do São Paulo (FAPESP) and Conselho

Nacional de Pesquisa (CNPq) to C.R.G., and from the UNICEF/UNDP/World Bank/WHO Special Programme for Research and Training in Tropical Diseases (TDR), ANPCyT, Fundación Florencio Fiorini and UNSAM to CAB.

#### **REFERENCES**

- 1 Moncayo, A. and Ortiz Yanine, M. I. (2006) An update on Chagas disease (human American trypanosomiasis). Ann. Trop. Med. Parasitol. 100, 663–677
- 2 Hotez, P. J., Bottazzi, M. E., Franco-Paredes, C., Ault, S. K. and Periago, M. R. (2008) The neglected tropical diseases of Latin America and the Caribbean: a review of disease burden and distribution and a roadmap for control and elimination. PLoS Negl. Trop. Dis. 2, e300
- 3 Tibayrenc, M. (2007) Human genetic diversity and the epidemiology of parasitic and other transmissible diseases. Adv. Parasitol. 64, 377–422
- 4 Zingales, B., Andrade, S. G., Briones, M. R., Campbell, D. A., Chiari, E., Fernandes, O., Guhl, F., Lages-Silva, E., Macedo, A. M., Machado, C. R. et al. (2009) A new consensus for *Trypanosoma cruzi* intraspecific nomenclature: second revision meeting recommends Tcl to TcVI. Mem. Inst. Oswaldo Cruz **104**, 1051–1054
- 5 Macedo, A. M. and Pena, S. D. (1998) Genetic variability of *Trypanosoma cruzi*: implications for the pathogenesis of Chagas disease. Parasitol. Today 14, 119–124
- 6 Buscaglia, C. A. and Di Noia, J. M. (2003) *Trypanosoma cruzi* clonal diversity and the epidemiology of Chagas' disease. Microbes Infect. 5, 419–427
- 7 Yoshida, N. (2006) Molecular basis of mammalian cell invasion by *Trypanosoma cruzi*. An. Acad. Bras. Cienc. **78**, 87–111
- 8 Villalta, F., Scharfstein, J., Ashton, A. W., Tyler, K. M., Guan, F., Mukherjee, S., Lima, M. F., Alvarez, S., Weiss, L. M., Huang, H. et al. (2009) Perspectives on the *Trypanosoma cruzi*-host cell receptor interactions. Parasitol. Res. **104**, 1251–1260
- 9 Epting, C. L., Coates, B. M. and Engman, D. M. (2010) Molecular mechanisms of host cell invasion by *Trypanosoma cruzi*. Exp. Parasitol. **126**, 283–291
- 10 Andrade, L. O. and Andrews, N. W. (2005) The *Trypanosoma cruzi*—host-cell interplay: location, invasion, retention. Nat. Rev. Microbiol. 3, 819–823
- Magdesian, M. H., Tonelli, R. R., Fessel, M. R., Silveira, M. S., Schumacher, R. I., Linden, R., Colli, W. and Alves, M. J. (2007) A conserved domain of the gp85/trans-sialidase family activates host cell extracellular signal-regulated kinase and facilitates *Trypanosoma cruzi* infection. Exp. Cell Res. 313, 210–218
- 12 Chuenkova, M. V. and PereiraPerrin, M. (2004) Chagas' disease parasite promotes neuron survival and differentiation through TrkA nerve growth factor receptor. J. Neurochem. 91, 385–394
- 13 Nde, P. N., Simmons, K. J., Kleshchenko, Y. Y., Pratap, S., Lima, M. F. and Villalta, F. (2006) Silencing of the laminin γ-1 gene blocks *Trypanosoma cruzi* infection. Infect. Immun. 74, 1643–1648
- 14 Staquicini, D. I., Martins, R. M., Macedo, S., Sasso, G. R., Atayde, V. D., Juliano, M. A. and Yoshida, N. (2010) Role of gp82 in the selective binding to gastric mucin during oral infection with *Trypanosoma cruzi*. PLoS Negl. Trop. Dis. 4, e613
- 15 Schenkman, S., Jiang, M. S., Hart, G. W. and Nussenzweig, V. (1991) A novel cell surface trans-sialidase of Trypanosoma cruzi generates a stage-specific epitope required for invasion of mammalian cells. Cell 65, 1117–1125
- 16 Turner, C. W., Lima, M. F. and Villalta, F. (2002) *Trypanosoma cruzi* uses a 45-kDa mucin for adhesion to mammalian cells. Biochem. Biophys. Res. Commun. 290, 29–34
- 17 Buscaglia, C. A., Campo, V. A., Frasch, A. C. and Di Noia, J. M. (2006) Trypanosoma cruzi surface mucins: host-dependent coat diversity. Nat. Rev. Microbiol. 4, 229–236
- 18 Augustine, S. A., Kleshchenko, Y. Y., Nde, P. N., Pratap, S., Ager, E. A., Burns, Jr, J. M., Lima, M. F. and Villalta, F. (2006) Molecular cloning of a *Trypanosoma cruzi* cell surface casein kinase II substrate, Tc-1, involved in cellular infection. Infect. Immun. 74, 3922–3929
- 19 Baida, R. C., Santos, M. R., Carmo, M. S., Yoshida, N., Ferreira, D., Ferreira, A. T., El Sayed, N. M., Andersson, B. and da Silveira, J. F. (2006) Molecular characterization of serine-, alanine-, and proline-rich proteins of *Trypanosoma cruzi* and their possible role in host cell infection. Infect. Immun. 74, 1537–1546
- 20 Scharfstein, J., Schmitz, V., Morandi, V., Capella, M. M., Lima, A. P., Morrot, A., Juliano, L. and Muller-Esterl, W. (2000) Host cell invasion by *Trypanosoma cruzi* is potentiated by activation of bradykinin B<sub>2</sub> receptors. J. Exp. Med. **192**, 1289–1300

Received 10 January 2012/15 March 2012; accepted 20 March 2012 Published as BJ Immediate Publication 20 March 2012, doi:10.1042/BJ20120074

- 21 Di Noia, J. M., Buscaglia, C. A., De Marchi, C. R., Almeida, I. C. and Frasch, A. C. (2002) A *Trypanosoma cruzi* small surface molecule provides the first immunological evidence that Chagas' disease is due to a single parasite lineage. J. Exp. Med. 195, 401–413
- 22 Bhattacharyya, T., Brooks, J., Yeo, M., Carrasco, H. J., Lewis, M. D., Llewellyn, M. S. and Miles, M. A. (2010) Analysis of molecular diversity of the *Trypanosoma cruzi* trypomastigote small surface antigen reveals novel epitopes, evidence of positive selection and potential implications for lineage-specific serology. Int. J. Parasitol. 40, 921–928
- 23 Buscaglia, C. A., Campo, V. A., Di Noia, J. M., Torrecilhas, A. C., De Marchi, C. R., Ferguson, M. A., Frasch, A. C. and Almeida, I. C. (2004) The surface coat of the mammal-dwelling infective trypomastigote stage of *Trypanosoma cruzi* is formed by highly diverse immunogenic mucins. J. Biol. Chem. 279, 15860–15869
- 24 De Marchi, C. R., Di Noia, J. M., Frasch, A. C., Amato Neto, V., Almeida, I. C. and Buscaglia, C. A. (2011) Evaluation of a recombinant *Trypanosoma cruzi* mucin-like antigen for serodiagnosis of Chagas' disease. Clin. Vaccine Immunol. 18, 1850–1855
- 25 Beraldo, F. H. and Garcia, C. R. (2005) Products of tryptophan catabolism induce Ca<sup>2+</sup> release and modulate the cell cycle of *Plasmodium falciparum* malaria parasites. J. Pineal Res. 39, 224–230
- 26 Urban, I., Santurio, L. B., Chidichimo, A., Yu, H., Chen, X., Mucci, J., Agüero, F. and Buscaglia, C. A. (2011) Molecular diversity of the *Trypanosoma cruzi* TcSMUG family of mucin genes and proteins. Biochem. J. 438, 303–313
- 27 Cordero, E. M., Nakayasu, E. S., Gentil, L. G., Yoshida, N., Almeida, I. C. and da Silveira, J. F. (2009) Proteomic analysis of detergent-solubilized membrane proteins from insect-developmental forms of *Trypanosoma cruzi*. J. Proteome Res. 8, 3642–3652
- 28 Almeida, I. C., Ferguson, M. A., Schenkman, S. and Travassos, L. R. (1994) Lytic anti-α-galactosyl antibodies from patients with chronic Chagas' disease recognize novel *O*-linked oligosaccharides on mucin-like glycosyl-phosphatidylinositol-anchored glycoproteins of *Trypanosoma cruzi*. Biochem. J. **304**, 793–802
- 29 Koyama, F. C., Chakrabarti, D. and Garcia, C. R. (2009) Molecular machinery of signal transduction and cell cycle regulation in *Plasmodium*. Mol. Biochem. Parasitol. 165, 1–7
- 30 Plotnikov, A., Zehorai, E., Procaccia, S. and Seger, R. (2011) The MAPK cascades: signaling components, nuclear roles and mechanisms of nuclear translocation. Biochim. Biophys. Acta 1813, 1619–1633
- 31 Aoki Mdel, P., Cano, R. C., Pellegrini, A. V., Tanos, T., Guinazu, N. L., Coso, O. A. and Gea, S. (2006) Different signaling pathways are involved in cardiomyocyte survival induced by a *Trypanosoma cruzi* glycoprotein. Microbes Infect. 8, 1723–1731
- 32 Manque, P. M., Neira, I., Atayde, V. D., Cordero, E., Ferreira, A. T., da Silveira, J. F., Ramirez, M. and Yoshida, N. (2003) Cell adhesion and Ca<sup>2+</sup> signaling activity in stably transfected *Trypanosoma cruzi* epimastigotes expressing the metacyclic stage-specific surface molecule gp82. Infect. Immun. 71, 1561–1565
- 33 Campo, V. A., Buscaglia, C. A., Di Noia, J. M. and Frasch, A. C. (2006) Immunocharacterization of the mucin-type proteins from the intracellular stage of *Trypanosoma cruzi*. Microbes Infect. 8, 401–409
- 34 Cimino, R. O., Rumi, M. M., Ragone, P., Lauthier, J., D'Amato, A. A., Quiroga, I. R., Gil, J. F., Cajal, S. P., Acosta, N., Juarez, M. et al. (2011) Immuno-enzymatic evaluation of the recombinant TSSA-II protein of *Trypanosoma cruzi* in dogs and human sera: a tool for epidemiological studies. Parasitology 138, 995–1002
- 35 D'Orso, I., De Gaudenzi, J. G. and Frasch, A. C. (2003) RNA-binding proteins and mRNA turnover in trypanosomes. Trends Parasitol. 19, 151–155
- 36 Wan, Y., Kertesz, M., Spitale, R. C., Segal, E. and Chang, H. Y. (2011) Understanding the transcriptome through RNA structure. Nat. Rev. Genet. 12, 641–655
- 37 Risso, M. G., Garbarino, G. B., Mocetti, E., Campetella, O., Gonzalez Cappa, S. M., Buscaglia, C. A. and Leguizamon, M. S. (2004) Differential expression of a virulence factor, the *trans*-sialidase, by the main *Trypanosoma cruzi* phylogenetic lineages. J. Infect. Dis. **189**, 2250–2259
- 38 Zingales, B., Souto, R. P., Mangia, R. H., Lisboa, C. V., Campbell, D. A., Coura, J. R., Jansen, A. and Fernandes, O. (1998) Molecular epidemiology of American trypanosomiasis in Brazil based on dimorphisms of rRNA and mini-exon gene sequences. Int. J. Parasitol. 28, 105–112
- 39 Miles, M. A., Feliciangeli, M. D. and de Arias, A. R. (2003) American trypanosomiasis (Chagas' disease) and the role of molecular epidemiology in guiding control strategies. Br. Med. J. 326, 1444–1448



## **SUPPLEMENTARY ONLINE DATA**

## Involvement of TSSA (trypomastigote small surface antigen) in Trypanosoma cruzi invasion of mammalian cells<sup>1</sup>

Gaspar E. CÁNEPA\*, Maria Sol DEGESE†, Alexandre BUDU‡, Celia R. S. GARCIA‡ and Carlos A. BUSCAGLIA\*2

\*Instituto de Investigaciones Biotecnológicas-Instituto Tecnológico de Chascomús (IIB-INTECh), Universidad Nacional de San Martín (UNSAM)—CONICET, Av. Gral Paz y Albarellos, Predio INTI, Edificio 24, San Martín, Buenos Aires, Argentina, †Instituto de Fisiología, Biología Molecular y Neurociencias (IFIBYNE), Facultad de Ciencias Exactas y Naturales, Universidad de Buenos Aires (UBA)—CONICET, Intendente Güiraldes 2160, Pabellón 2, Ciudad Universitaria, Buenos Aires, Argentina, and ‡Universidade de São Paulo, Departamento de Fisiologia, Instituto de Biociências, Cidade Universitária, 05508-900 São Paulo, Brazil

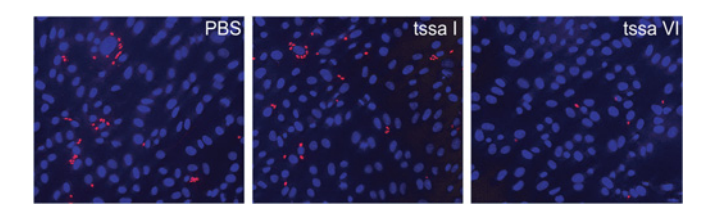


Figure S1 TSSA is involved in parasite internalization

Representative low-magnification ( $\times$ 40) images of CL Brener cell-derived trypomastigote infection experiments on Vero cell monolayers in the presence of PBS, tssa I or tssa VI peptide. Intracellular parasites are stained in red and Vero cell nuclei are counterstained with DAPI (blue).

Table S1 Oligonucleotides used in the present study

Sequence $(5' \rightarrow 3')$
TCTAGAATGACTACGTGCCGTCTGCTG ATCGATCCCCGGTTGAGATGGAGCTT ATCGATTCCCGATGGAGGATGGA GAATTCTCTTTCAGGTGAAGCAGAAGCC AAGCTTTCAGGCCAGAGAGGCGGTGTA CAATATAGTACAGAAACTGTATCAATAATAGGGTT GCGAGCTCCGCGGCCGCGTTTTTTTTTT

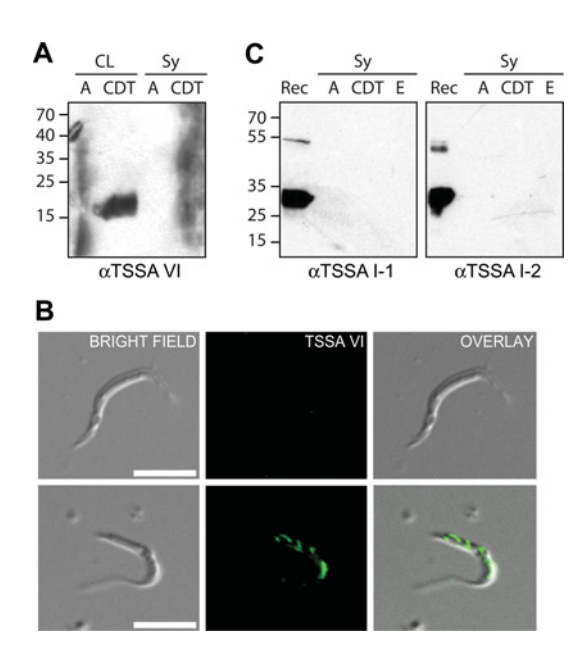


Figure S2 Lack of cross-reactivity between TSSA isoforms

(A) Cell-derived trypomastigote (CDT) and extracellular amastigote (A) forms (107) of CL Brener (CL) or Sylvio X-10 (Sy) parasite stock were analysed by Western blotting probed with purified anti-(TSSA VI) Abs (1:2000 dilution). Molecular masses are indicated in kDa. (B) Sylvio X-10 (upper panels) or CL Brener (lower panels) cell-derived trypomastigote forms were analysed by indirect IFA probed with anti-TSSA VI purified Abs (1:500 dilution). Scale bars, 10  $\mu$ m. (C) Epimastigote (E), cell-derived trypomastigote (CDT) and extracellular amastigote (A) forms (107) of Sylvio X-10 (Sy) parasite stock were analysed by Western blotting probed with two different mouse antisera raised against GST–TSSA I (1:500 dilution). The recombinant GST–TSSA I protein (Rec, 1.5  $\mu$ g) was loaded as a control. Molecular masses are indicated in kDa.

<sup>&</sup>lt;sup>1</sup> This paper is dedicated to the memory of Dr Rodolfo Ugalde.

<sup>&</sup>lt;sup>2</sup> To whom correspondence should be addressed (email cbusca@iib.unsam.edu.ar).

The cDNA sequence data reported for trypomastigote small surface antigen I (TSSA I) have been deposited in the DDBJ, EMBL, GenBank® and GSDB Nucleotide Sequence Databases under accession number JQ354939.

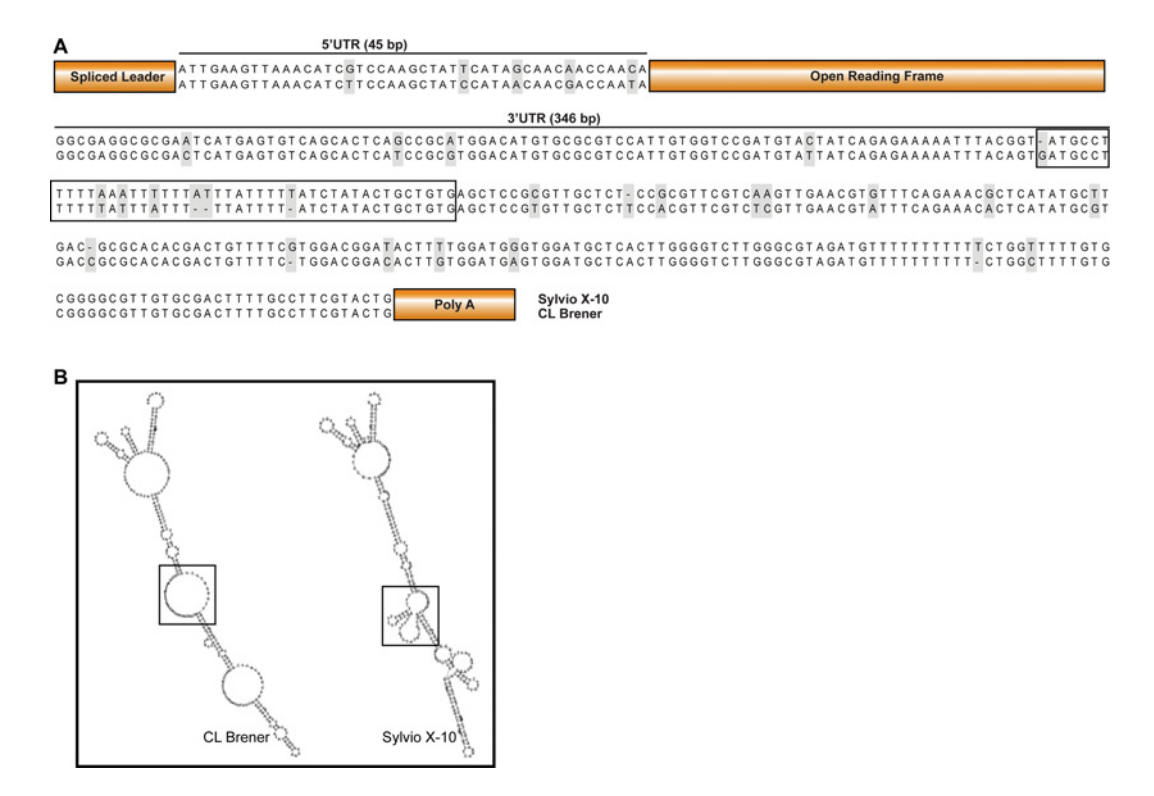


Figure S3 Sequence and structural features of TSSA I mRNA

(A) Schematic representation of *TSSA I* mRNA isolated from Sylvio X-10 cell-derived trypomastigote forms (GenBank® accession number JQ354939). Sequences from 5'- and 3'-UTRs are indicated and compared with those of *TSSA VI* mRNA isolated from CL Brener parasites (GenBank® accession numbers AF036421 and AF036443). Variable positions are shaded. (B) Secondary-structure prediction and graphical outputs of the 3'-UTRs were obtained using RNAfold Web Server (http://rna.tbi.univie.ac.at). A putative destabilizing-like hairpin-and-loop structure [1] present in the Sylvio X-10 3'-UTR, but absent from the CL Brener 3'-UTR is boxed.

### REFERENCE

1 Wan, Y., Kertesz, M., Spitale, R. C., Segal, E. and Chang, H. Y. (2011) Understanding the transcriptome through RNA structure. Nat. Rev. Genet. 12, 641–655

Received 10 January 2012/15 March 2012; accepted 20 March 2012 Published as BJ Immediate Publication 20 March 2012, doi:10.1042/BJ20120074